Microphotoluminescence of exciton and biexciton around 1.5μm from a single InAs/InP(001) quantum dot

G. Saint-Girons, Nicolas Chauvin, A. Michon, G. Patriarche, G. Beaudoin, G. Bremond, C. Bru-Chevallier, I. Sagnes

Microphotoluminescence of exciton and biexciton around 1.5 μm from a single InAs/InP(001) quantum dot

G. Saint-Girons[a)]
LPN, UPR-CNRS, 20 Route de Nozay, 91460 Marcoussis, France

N. Chauvin
LPM, UMR-CNRS, INSA-Lyon, 69621 Villeurbanne, France

A. Michon, G. Patriarche, and G. Beaudoin
LPN, UPR-CNRS, 20 Route de Nozay, 91460 Marcoussis, France

G. Brémond and C. Bru-Chevallier
LPM, UMR-CNRS, INSA-Lyon, 69621 Villeurbanne, France

I. Sagnes
LPN, UPR-CNRS, 20 Route de Nozay, 91460 Marcoussis, France

(Received 26 October 2005; accepted 13 February 2006; published online 27 March 2006)

We report on the fabrication by low-pressure metalorganic vapor phase epitaxy of InAs/InP(001) quantum dots (QDs) emitting around 1.5 μm, and on the observation of microphotoluminescence (μPL) from a single QD in this wavelength range. The QDs are diamond shaped, with a density of $6.3 \cdot 10^9$ cm^{-2}. μPL experiments were carried out on a QD sample covered with a gold mask containing apertures (diameter of 200 nm). Well defined peaks corresponding to the emission of single QDs were recorded between 1.24 and 1.6 μm. The analysis of the pump power dependence of their intensity allows us to discriminate between exciton and biexciton emission lines. © *2006 American Institute of Physics*. [DOI: 10.1063/1.2185008]

The development of fiber-based quantum cryptography communication systems requires the realization of efficient single photon sources emitting around 1.5 μm. Recent progresses in the Stranski–Krastanov growth of self-assembled quantum dots (QDs) have given rise to a wide range of studies concerning the optical properties of single QDs.[1–3] It has been demonstrated that due to their discrete density of electronic states, these nanostructures could be efficiently used to produce single photon emission. Antibunching experiments carried out on In(Ga)As/GaAs QDs emitting around 1 μm have evidenced the promising properties of the QDs for the realization of single photon sources.[4–6] More recently, microphotoluminescence (μPL) experiments have been carried out on CdSe/ZnSe (around 540 nm),[7] GaN/AlN (around 500 nm),[8] or CdTe/ZnTe (around 485 nm)[9] QDs. However, only a few works have been reported concerning μPL studies of QDs emitting at 1.3 and 1.5 μm. This is partly due to the difficulty in realizing sensitive and low-noise detection systems in this spectral region, and to fabricate low-density QD arrays emitting in this wavelength range. Alloing *et al.*[10] have developed an original growth sequence that allows the molecular beam epitaxy (MBE) of low density In(Ga)As/GaAs QDs emitting at 1.3 μm, and they have recently observed μPL from a single QD at this wavelength. The fabrication of single photon sources at longer wavelength requires the use of InAs/InP QDs, whose emission can be tuned around 1.5 μm. However, various studies involving MBE[11] and chemical beam epitaxy[12] growth of InAs QDs on exactly (001)-oriented InP substrates demonstrate the difficulty in obtaining real three-dimensional QDs using these high-vacuum growth techniques. On the other hand, a few works[13] indicate that metalorganic vapor phase epitaxy (MOVPE) allows the fabrication of well defined QDs. Very recently, Takemoto *et al.*[14] have observed a μPL signal around 1.5 μm from a single InAs/InP QD grown by MOVPE corresponding to the exciton emission line.

In this letter, we report the fabrication of high optical efficiency InAs/InP(001) QDs grown by low-pressure MOVPE and the observation by power-dependent μPL of well defined exciton and biexciton lines around 1.5 μm from a single QD.

The sample studied in the following was grown in a vertical low-pressure MOVPE system using hydrogen as a carrier gas and standard precursors [arsine, phosphine, and trimethylindium (TMI)], at a work pressure of 60 Torr. The growth sequence is as follows: after a 150 nm thick InP buffer layer deposited at 625 °C on an exactly (001)-oriented InP substrate, the growth temperature is lowered to 530 °C for the QD deposition. The QDs are formed by depositing 4 monolayers (ML) of InAs, at a growth rate of 0.3 ML s^{-1} (TMI flow rate of 0.23 μmol s^{-1}). Finally, a 40 nm thick InP capping layer is grown over the QDs at 530 °C.

For the μPL experiments, the sample was masked with a gold layer containing apertures (diameter ≈200 nm). μPL was excited using the 632.8 nm emission line of a He–Ne laser, focused onto a 3 μm diam spot by a microscope objective. The μPL signal was collected through the same objective, and detected by a nitrogen cooled InGaAs array detector after dispersion in a grating monochromator.

A transmission electron microscopy (TEM) plane view of the sample taken under 001 zone-axis bright field condition is shown in Fig. 1. It contains well-defined three-dimensional dislocation-free QDs, with a density of $6.3 \cdot 10^9$ cm^{-2}. This density is approximately three times

a)Electronic mail: guillaume.saint-girons@lpn.cnrs.fr

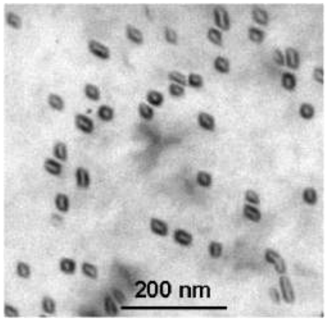

FIG. 1. TEM plane view of the sample taken under 001 zone-axis bright-field condition. The QDs are diamond shaped, and present a density of $6.3 \cdot 10^9$ cm^{-2}. The dark contrast corresponds to the highly strained base of the QDs.

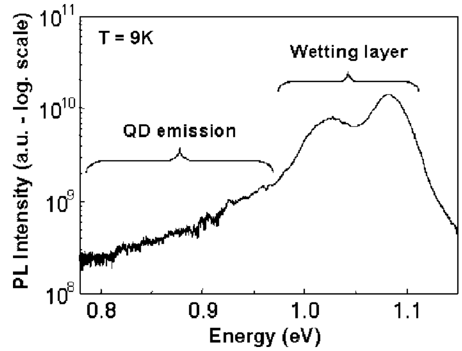

FIG. 3. Standard PL spectrum of the sample recorded at 9 K with an excitation power density of 0.3 W cm^{-2}.

lower than the density reported in Ref. 14. In our growth conditions, the QD density is mainly driven by the growth rate, and can be precisely controlled between a few 10^8 and a few 10^{10} cm^{-2} by varying the incident TMI flow rate. Detailed views of a typical QD are shown in Fig. 2. It is diamond shaped, slightly elongated along the [1–10] direction, with edges along the [1–30] and [3–10] directions. The same type of geometry, which origin remains unclear, has recently been observed[15] in the case of uncapped InAs/InP QDs. The average largest dimension of the QDs (along [1–10]), calculated over approximately 110 QDs, is 43 nm, and their average smallest dimension (along [110]) is 23 nm. The QDs present a flat shape [TEM cross view of Fig. 2(b)], and exhibit an average height of 2.1 nm (including the wetting layer, whose thickness is close to 0.8 nm), with a height dispersion of ±0.8 nm.

A standard photoluminescence (PL) spectrum of the sample, recorded at 9 K under low excitation power (0.3 W cm^{-2}), is shown in Fig. 3. The PL of the QDs covers a wide energy range between 0.78 eV (1.6 μm) and 1 eV (1.24 μm). Above 1 eV, the spectrum exhibits well defined peaks that we attribute to the emission of the wetting layer presenting monolayer height fluctuations. The PL intensity of the wetting layer is between 1 and 2 orders of magnitude larger than the one of the QDs. This is related to the relatively low QD density and to a reduced carrier diffusion length at low temperature that reduce the charge carrier capture efficiency of the QDs at 9 K. PL spectra of the same sample recorded at higher temperature (77 and 300 K, not shown here) exhibit well resolved peaks corresponding to the emission of QDs with heights varying by discrete steps of 1 monolayer, as already observed in 14 and in several other studies. μPL spectra were recorded at 9 K through one of the apertures of the gold mask. This mask spatially isolates approximately three QDs. The spectral filtering performed by the monochromator allows selecting the μPL signal of each single QD. The μPL spectra shown in Fig. 4 were recorded under various excitation powers (P). Note that similar μPL spectra were observed in the entire emission range of the QDs, which is between 1.24 and 1.6 μm. For $P=60$ μW, the spectrum exhibits a single emission line at 821.5 meV (labeled X), with a full width at half maximum (FWHM) of 150 μeV, limited by the resolution of our setup. For P larger than 0.2 mW, a second emission line (labeled $2X$) arises at 820.9 meV. The evolution of the integrated intensity of these two lines while increasing the pump power P is plotted in Fig. 5. For $P < 200$ μW, the intensity of the X line (circle in the figure) increases as P, while the intensity of the $2X$ line increases as P^2. The behavior of the X line is typical for the radiative recombination of a single exciton trapped in the QD, while the $2X$ line corresponds to the radiative recombination of an exciton when the QD contains two excitons (biexciton line). For $P > 200$ μW (respectively, 580 μW), the intensity of the X (respectively $2X$ line) saturates, and

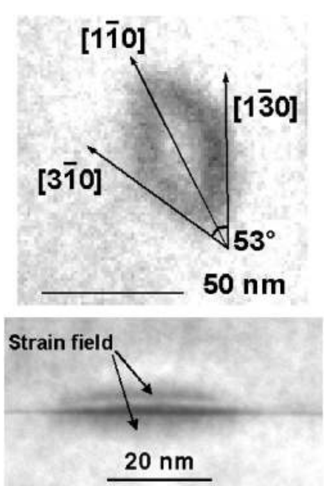

FIG. 2. (a) Close view of a single QD. It presents a slight elongation along the [1–10] direction, and the edges are oriented along the [3–10] and [1–30] directions. (b) TEM cross view of a QD. The average height of the QDs is 2.1 nm, and the thickness of the wetting layer is 0.8 nm. The dark contrast around the QD corresponds to the strain field surrounding the nanostructure.

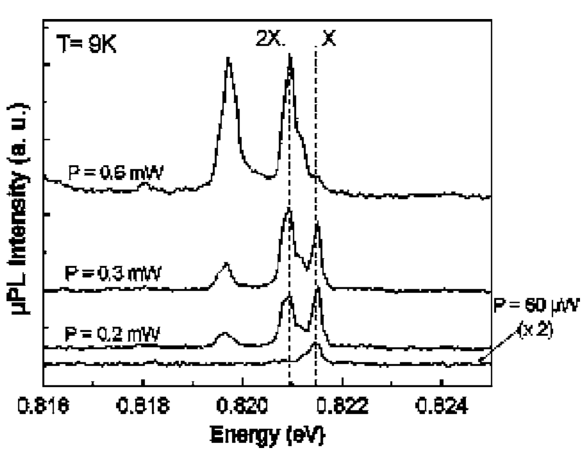

FIG. 4. μPL spectrum of a single QD recorded at 9 K under various excitation powers between 60 μW and 0.6 mW. The X and $2X$ lines correspond to the radiative recombination of the exciton and the biexciton, respectively.

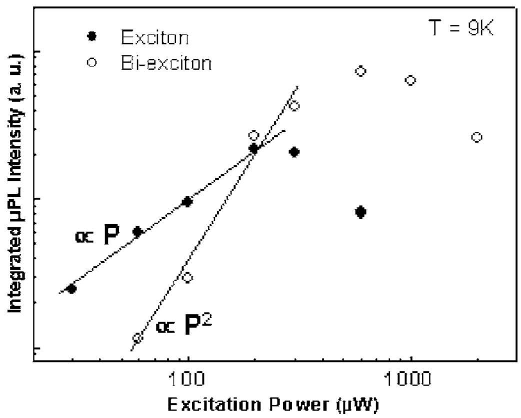

FIG. 5. Power dependence of the integrated μPL intensity of the X (full circle) and $2X$ (open circle) lines. Log scale in abscissa and ordinate: (full lines) fit of the experimental data with a linear (respectively, square) function of the pump power for the X (respectively, $2X$) line.

then decreases while increasing P. This behavior is related to the evolution with P of the probability of having one (p_1), two (p_2), or more $(p_{>2})$ electron-hole pairs in the QD:For $P < 200\ \mu$W, p_1 is larger than p_2 and $p_{>2}$ and the X line dominates the spectrum. For $200\ \mu\text{W} < P < 580\ \mu$W, p_2 becomes larger than p_1, leading to a reduction of the X line intensity at the benefit of the $2X$ line. For $P > 580\ \mu$W the probability of having more than two electron-hole pairs in the QD becomes larger than p_1 and p_2, leading to further reduction of the intensities of the X and $2X$ lines. The binding energy of the biexciton is 0.6 meV. This value is of the same order of magnitude as the ones reported in the literature.[16,17] In Ref. 18, the authors theoretically derive a binding energy of 1.4 meV for InAs/InP QDs with an average lateral size of 35 nm. This value is similar to the one deduced from our experiments.

We fabricated defect-free InAs/InP(001) QDs emitting around 1.5 μm by low pressure MOVPE, and we clearly observed the radiative recombination of exciton and biexciton in a single QD by μPL at 9 K. Comparable studies have been reported in Ref. 14. In this earlier work however, the authors do not observe the radiative recombination of biexcitons in the QD. Moreover, they use a high density $(1.8 \times 10^{10}\ \text{cm}^{-2})$ QD ensemble that implies the development of a rather complicated mesa technology to isolate a single QD. In comparison, our lower QD density facilitates single QD spectroscopy experiments and is more suitable for the fabrication of single dot devices. The results presented here demonstrate the high potential of the MOVPE grown InAs/InP(001) QDs for the realization of single photon emitters around 1.5 μm. They also open the way to further spectroscopic studies of these nanostructures, enlarging the field of the μPL experiments on QDs to the very important wavelength range of the telecommunication systems.

The authors gratefully thank J. Y. Marzin, S. Varoutsis, and S. Laurent for useful discussions. This work was supported by the SANDIE EC Network of Excellence, by SESAME Project No. 1377, by the Région Ile de France, and by the Conseil Général de l'Essonne.

[1] J.-Y. Marzin, J.-M. Gérard, A. Izraël, D. Barrier, and G. Bastard, Phys. Rev. Lett. **73**, 716 (1994).
[2] E. S. Moskalenko, V. Donchev, K. F. Karlsson, P. O. Holtz, B. Monemar, W. V. Schoenfeld, J. M. Garcia, and P. M. Petroff, Phys. Rev. B **68**, 155317 (2004).
[3] C. Kamerer, G. Cassabois, C. Voisin, G. Delalande, Ph. Roussignol, and J. M. Gérard, Phys. Rev. Lett. **87**, 207401 (2001).
[4] E. Moreau, I. Robert, J. M. Gérard, I. Abram, L. Manin, and V. Thierry-Mieg, Appl. Phys. Lett. **79**, 2865 (2001).
[5] P. Michler, A. Kiraz, C. Becher, W. V. Schoenfeld, P. M. Petroff, L. Zhang, E. Hu, and A. Imamoglu, Science **290**, 2282 (2000).
[6] J. Hours, S. Varoutsis, M. Gallart, J. Bloch, I. Robert-Philip, A. Cavanna, I. Abram, F. Laruelle, and J. M. Gérard, Appl. Phys. Lett. **82**, 2206 (2003).
[7] B. Patton, W. Langbein, and U. Woggon, Phys. Rev. B **68**, 125316 (2003).
[8] S. Kako, K. Hoshino, S. Iwamoto, S. Ishida, and Y. Arakawa, Appl. Phys. Lett. **85**, 64 (2004).
[9] C. Couteau, S. Moehl, F. Tinjod, J. M. Gérard, K. Kheng, H. Mariette, J. A. Gaj, R. Romestain, and J. P. Poizat, Appl. Phys. Lett. **85**, 6251 (2004).
[10] B. Alloing, C. Zinoni, L. H. Li, C. Monat, M. Gobet, G. Buchs, A. Fiore, E. Pelucchi, and E. Kapon, Appl. Phys. Lett. **86**, 101908 (2005).
[11] M. Gendry, C. Monat, J. Brault, P. Regreny, G. Hollinger, B. Salem, G. Guillot, T. Benyattou, C. Bru-Chevallier, G. Bremond, and O. Marty, J. Appl. Phys. **95**, 4761 (2004).
[12] P. J. Poole, J. McCaffrey, R. L. Williams, J. Lefebvre, and D. Chthrani, J. Vac. Sci. Technol. B **19**, 1467 (2001).
[13] B. Wang, F. Zhao, Y. Peng, Z. Jin, Y. Li, and S. Liu, Appl. Phys. Lett. **72**, 2433 (1998).
[14] K. Takemoto, Y. Sakuma, S. Hirose, T. Usuki, and N. Yokoyama, Jpn. J. Appl. Phys., Part 2 **43**, L349 (2004).
[15] H. Hwang, S. Yoon, H. Kwon, E. Yoon, H.-S. Kim, J. Y. Lee, and B. Cho, Appl. Phys. Lett. **85**, 6383 (2004).
[16] S. Rodt, R. Heitz, A. Schliwa, R. L. Sellin, F. Guffarth, and D. Bimberg, Phys. Rev. B **68**, 035331 (2003).
[17] D. Chithrani, R. L. Williams, J. Lefebvre, P. J. Poole, and G. C. Aers, Appl. Phys. Lett. **84**, 978 (2004).
[18] W. Sheng and P. Hawrylak, Phys. Rev. B **72**, 035326 (2005).